Chemical Science

ROYAL SOCIETY OF CHEMISTRY

EDGE ARTICLE

View Article Online
View Journal | View Issue

Cite this: *Chem. Sci.*, 2024, **15**, 20503

All publication charges for this article have been paid for by the Royal Society of Chemistry

Received 10th October 2024
Accepted 11th November 2024

DOI: 10.1039/d4sc06902a

rsc.li/chemical-science

Direct ladderization of cyclooctatetraene-containing, processable conjugated ladder polymers from annulated bis-zirconacyclopentadienes†

August J. Rothenberger, [a] Harrison M. Bergman, [a] He Li, [bc] Miao Qi, [b] Yunfei Wang, [b] Yi Liu *[bc] and T. Don Tilley *[ad]

Conjugated ladder polymers (CLPs) are difficult yet captivating synthetic targets due to their fully unsaturated fused backbones. Inherent challenges associated with their synthesis often lead to low yields, structural defects, and insoluble products. Here a new method to form CLPs is demonstrated, utilizing a high-yielding dimerization of annulated zirconacyclopentadienes to form cyclooctatetraene (COT) monomer units. The resulting COT-containing polymers form rapidly in a single ladderization step from the bis-zirconacyclopentadiene precursors and display M_n up to 29.7 kg mol^{-1}. The polymers represent rare examples of CLPs with negatively curved rings, resulting in the observation of unusual properties. The rigid tub-shaped COT units embedded in the backbone imbue the polymers with microporosity, exhibiting BET surface areas up to 555 m^2 g^{-1}. Additionally, the remarkable solubility of these CLPs in organic solvents enables the fabrication of thin films showcasing high dielectric performance with a discharged energy density as high as 6.54 J cm^{-3} at 650 MV m^{-1}.

Introduction

Ladder polymers are an intriguing class of materials where the polymer chain consists of multiple backbones connected at regular intervals like the rungs of a ladder.[1,2] These polymers are generally rigid and can display disordered packing resulting in intrinsic microporosity[3,4] that allows applications as membranes with high thermal stability[5] and remarkable gas selectivity.[6] A subset class of ladder polymer, conjugated ladder polymers (CLPs, also known as fully unsaturated ladder polymers) have a fully sp^2-hybridized backbone and are of interest due to the electronic properties that arise from their partially delocalized electrons.[7–11] However, CLPs are difficult to synthesize, particularly in high yields and with large molecular weights, as a result of the inherent difficulty of forming many fused rings. Additionally, many CLPs are sparingly soluble, further hindering their synthesis, characterization, and processing.

The use of negatively-curved rings to form contorted and flexible nanographene materials has been the topic of many recent studies,[12–17] but their use in CLPs is less explored.[18] To date, there are still no methods of generating negatively curved rings in high enough yield for the synthesis of high molecular weight CLPs. Müllen and co-workers first incorporated eight-membered rings into graphene nanoribbons of M_n = 2.1 kg mol^{-1} *via* Ullmann coupling (Fig. 1a),[19] although these rings are planar and did not display the characteristic "tub-shape" of cyclooctatetraene (COT), possessing greater similarity to a biphenylene sheet.[20] A similar perylene diimide (PDI) nanoribbon was synthesized by Zhong on an Au(111) surface.[21] Recently, Jiang reported the use of Ullmann coupling to generate chiral PDI dimers and tetramers containing negatively curved eight-membered rings with high dissymmetry.[22] This iterative approach to the synthesis of oligomers highlights the inherent challenges of generating linear COT-containing ladder polymers. In 2023, Coskun synthesized a three-dimensional polymer network containing COT and biphenylene moieties *via* benzyne dimerization (Fig. 1b).[23] This initially generates a mostly linear biphenylene polymer, with appreciable COT crosslinks only being introduced during a separate thermal treatment at 400 °C to induce an intermolecular rearrangement of the polymer backbone. The resulting polymer is insoluble, limiting characterization of molecular weight or the efficiency

[a]*Department of Chemistry, University of California, Berkeley, California, 94720, USA. E-mail: tdtilley@berkeley.edu*

[b]*Molecular Foundry, Lawrence Berkeley National Laboratory, Berkeley, California, 94720, USA. E-mail: yliu@lbl.gov*

[c]*Materials Sciences Division, Lawrence Berkeley National Laboratory, Berkeley, California, 94720, USA*

[d]*Chemical Sciences Division, Lawrence Berkeley National Laboratory, Berkeley, California, 94720, USA*

† Electronic supplementary information (ESI) available. See DOI: https://doi.org/10.1039/d4sc06902a

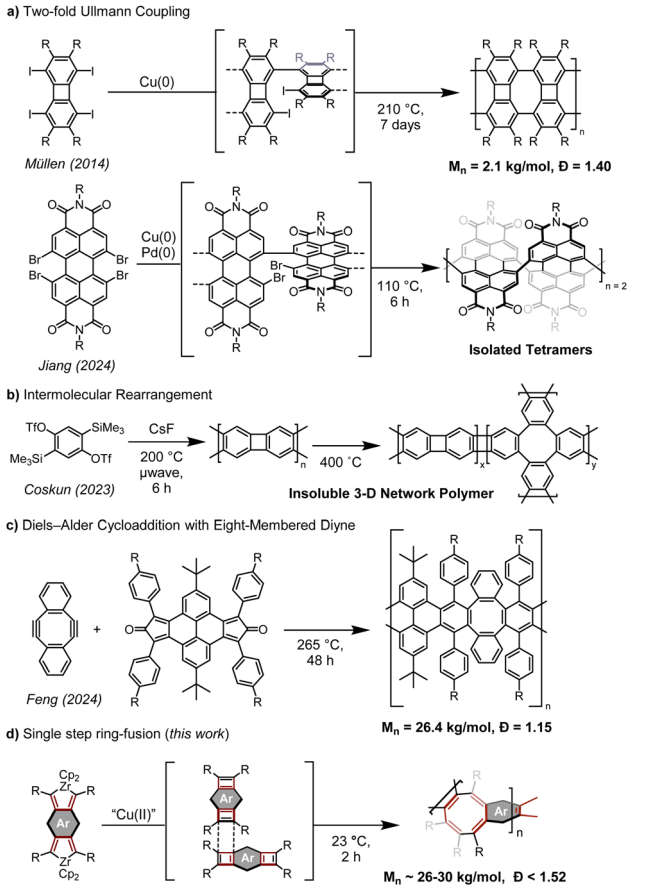

Fig. 1 (a) Ullmann coupling of aryl halides to yield planar eight-membered rings and tub-shaped COT-containing tetramers; (b) benzyne dimerization to yield COT-containing network polymers; (c) Diels–Alder cycloaddition of diyne and bis-cyclopentadienone, M_n and $Đ$ were determined after purification by recycling SEC; (d) dimerization of bis-zirconacycles.

of the COT generation step. The materials displayed high surface areas and gas absorption selectivity, showing promise for membrane applications of COT-containing materials.

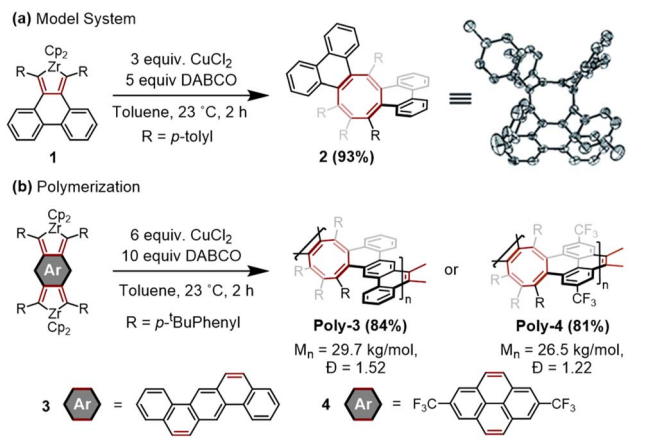

Scheme 1 (a) Synthesis of COT **2** from zirconacycle **1**. (b) COT-containing polymers **Poly-3** and **Poly-4** from bis-zirconacycle precursors **3** and **4**.

During the preparation of this manuscript, Feng and co-workers reported the synthesis of a ladder polymer by cycloaddition of a bis-cyclopentadienone with a cycloocta-1,5-diyne at 265 °C (Scheme 1c).[24] The success of this approach is predicated on the use of established Diels–Alder chemistry,[25,26] which requires a pre-made COT building block to install negative curvature. Additionally, the high M_n ~26.4 kg mol^{-1} and low dispersity of 1.15 are achieved after separation of fractions by recycling size exclusion chromatography. In each of the former cases, molecular weight and defect density are non-ideal due to COT formation occurring *via* two distinct reactions, either *via* successive Ullmann couplings or an intermolecular rearrangement. The development of approaches that utilize a single, concerted step to generate COT promises to circumvent these issues.

Such a reaction to generate a COT ring was previously described by this research group, whereby phenanthrene-annulated zirconacyclopentadiene (zirconacycle) **1** is converted to COT **2** *via* a cyclobutadiene intermediate at room temperature (Scheme 1a).[27] It is hypothesized that this occurs by dimerization of two transient phenanthrocyclobutadienes through a [4 + 2] cycloaddition and spontaneous rearrangement, affording a COT ring rapidly at room temperature. In this report we improve the efficiency of the reaction to enable its use for polymerization to obtain two COT-containing CLPs with different aromatic backbones, each displaying high molecular weight (M_n > 26 kg mol^{-1}) and low dispersity ($Đ \leq 1.52$) (Scheme 1b). Both resulting polymers are highly soluble in common organic solvents, enabling the fabrication of thin films as high-performance dielectrics.

Results and discussion

Cyclooctatetraene polymers **Poly-3** and **Poly-4** were synthesized in a single step by reaction of bis-zirconacycle precursors **3** and **4** with $CuCl_2$ and 1,4-diazobicyclo[2.2.2]octane (DABCO) (Scheme 1b). The polymers differ in the aromatic group annulated to the COT units, either disubstituted[*c*,*j*]dibenz[*a*,*h*]anthracene or disubstituted[*e*,*l*]2,7-di(trifluoromethyl)pyrene. The ligand DABCO was chosen after screening a variety of Lewis bases for the dimerization of **1** and optimization of the yield of **2** (Table S1†). The polymerization reaction is scalable and efficient, giving the polymers in 84% and 81% yields on a 200 mg scale, respectively. To probe the polymerization process, aliquots from the reaction of **Poly-3** were quenched with methanol at regular intervals and analyzed by size exclusion chromatography (SEC). After the polymerization begins, **Poly-3** rapidly increases in molecular weight, ultimately forming chains with maximum $M_n = 29.7$ kg mol^{-1} and $Đ = 1.52$ (Fig. 2a and b). The polymerization that yields **Poly-4** operates similarly, with a maximum $M_n = 26.5$ kg mol^{-1} with $Đ = 1.22$ within 2 h (Fig. S9 and S10†).

The polymers were also characterized by matrix-assisted laser desorption ionization-time of flight (MALDI-TOF) mass spectrometry, which gave molecular weights consistent with those determined by SEC analysis. **Poly-3** displays a prominent repeat unit of 854 *m*/*z* corresponding to the mass of the

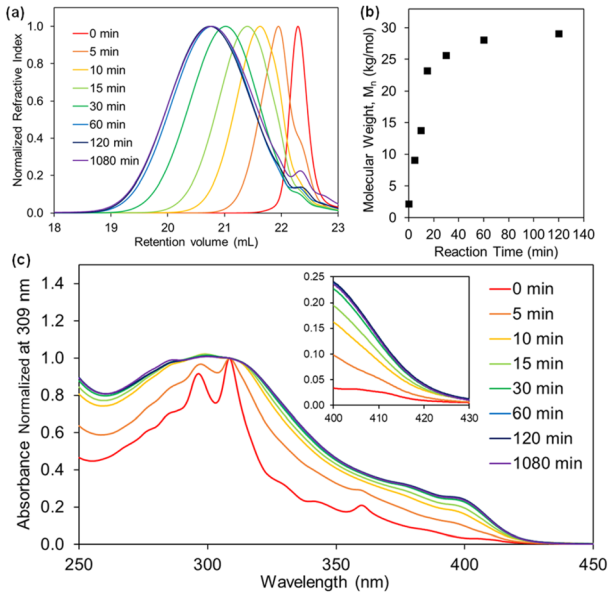

Fig. 2 (a) Normalized SEC curves of samples of **Poly-3** quenched at different time intervals; (b) plot of calculated molecular weight of **Poly-3** against reaction time; (c) UV-vis spectra of **Poly-3** obtained at different reaction times (normalized at maximum absorbance peak at 309 nm). The inset is the zoom-in of the absorption edge.

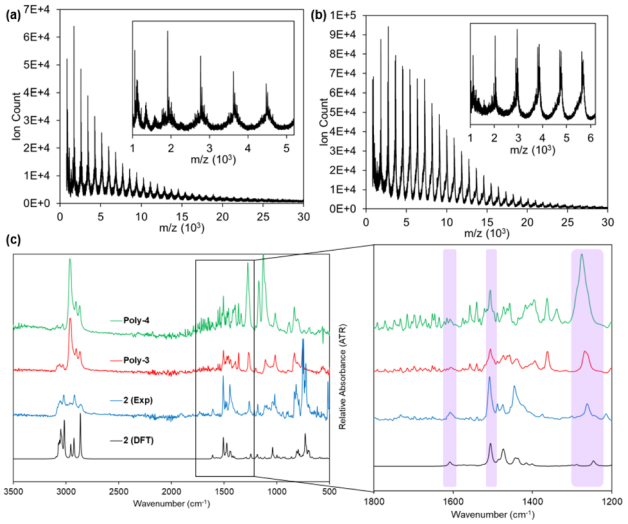

Fig. 3 (a) MALDI-TOF mass spectrum of **Poly-3**; (b) MALDI-TOF mass spectrum of **Poly-4**; (c) infrared absorbance spectra of **2** (DFT and experimental), **Poly-3**, and **Poly-4** (representative COT vibrations highlighted in purple).

monomer unit visible to about $X_n = 26$ (Fig. 3a). Similarly, the MALDI-TOF pattern for **Poly-4** possesses a 914 m/z repeat unit visible until $X_n = 28$ (Fig. 3b). Infrared spectroscopy was utilized to confirm the presence of cyclooctatetraene moieties in the backbone of the polymers. The spectra of **2**, **Poly-3**, and **Poly-4** were compared to a simulated IR spectrum of **2** calculated at the B3LYP/6-31g level of theory. Representative COT vibrations were found at 1606, 1504, and 1241 cm^{-1} (Fig. 3c) across all spectra, demonstrating shared COT functionality between **2**, **Poly-3**, and **Poly-4**.

The polymers display broad resonances in NMR spectra, due to the unsymmetrical substitution for the COT repeat unit. This is reflected in the ^{1}H NMR spectrum of monomeric **2**, which has 24 unique aryl proton resonance peaks.[28] Introduction of repeat units leads to further complexity; thus, the ratio of aryl to alkyl resonances is more informative. For both polymers, the resonance ratio nearly matches the predicted values of 1 : 1.38 for **Poly-3** and 1 : 1.80 for **Poly-4** (Fig. S1 and S3†). The ^{13}C NMR spectra are similarly broad for both polymers, with peaks in the aryl region between 155 to 125 ppm and resonances for alkyl groups between 35 and 30 ppm. Very few other peaks are visible in the ^{1}H spectrum of **Poly-3** at 3.43 and 3.28 ppm, indicating a highly selective polymerization with minimal defects. Similarly, in the ^{1}H spectrum of **Poly-4**, small defect peaks are present at 2.98 and 2.13 ppm. These likely correspond to annulated cyclobutene resonances, a plausible source of quenched chain ends.

UV-vis spectroscopy was utilized to determine the absorption onset for samples of **Poly-3** with increasing molecular weight (Fig. 2c). Normalized at the maximum absorbance peak for the sample of monomer **3** quenched before exposure to $CuCl_2$/DABCO (labeled as 0 min) the samples show a red-shifted absorption onset as M_n increases up to about 14 kg mol^{-1} at 15 min, indicating that the effective conjugation length along the polymer backbone occurs between 11–16 repeat units. Similarly, a red shift is observed in the absorption onset for **Poly-4** samples (Fig. S13†), corresponding to a maximum between 12–18 repeat units. Samples of COT **2**, **Poly-3**, and **Poly-4** are weakly fluorescent, displaying emission peaks at 455, 474, and 489 nm, respectively (Fig. S12†).

The incorporation of negatively curved COT rings embedded in a rigid ladder backbone makes **Poly-3** and **Poly-4** promising candidates as polymers with high intrinsic porosity.[29] The polymers were subjected to nitrogen adsorption measurements at 77 K and showed substantial uptake at low relative pressure (P/P_0). The calculated apparent Brunauer–Emmett–Teller surface areas (SA_{BET})[30] of 421 m^2 g^{-1} and 555 m^2 g^{-1} for **Poly-3** and **Poly-4** indicate that the polymers possess significant microporosity (Fig. S20†). Evaluation of pore sizes in the two polymers with non-local density functional theory (NLDFT) using a carbon-slit model revealed a microporous region with pores between 10.9–13.5 Å as well as some mesoporosity extending to pore diameters of 120–220 Å (Fig. S21 and S22†). Microporosity likely results from the negative curvature of the rigid COT monomer units forcing inefficient packing of polymer chains while the meso- to macroporosity may result from void space between polymer particles. The polymers have surface area metrics similar to other COT-containing networks,[23] but are noteworthy due to their ideal solution processibility amenable to castings of thin films.

The rigid structures of **Poly-3** and **Poly-4** imbues them with high thermal stability, such that they display relatively high decomposition temperatures around 350 and 325 °C, respectively, as measured by thermal gravimetric analysis (Fig. S14 and S15†). Neither possesses observable glass transition

temperatures within the thermally accessible range (Fig. S16 and S17†). Additionally, neither polymer displays reversible redox events as determined by cyclic voltammetry (Fig. S19†). This is consistent with the behavior of monomer **2**, which shows four irreversible reductions between −2.2 and −3.5 V *vs.* Fc/Fc^+ (Fig. S18†). The inability to access an aromatic COT dianion showcases the polymers' resistance to planarization and deformation of the polymeric structure.

The solution processability, thermal stability, and wide window of redox stability prompted us to consider these polymers as thin film-based dielectric materials for energy storage applications,[31–33] for which ladder polymers have been identified as promising candidates.[34,35] Indium tin oxide (ITO) coated glass substrates served as the conducting substrate (see ESI for casting procedure†). The films were analyzed by grazing-incidence wide-angle X-ray scattering (GI-WAXS) to reveal an amorphous distribution of polymer chains (Fig. S23†).

At 10^3 Hz, films of **Poly-3** exhibit a dielectric constant of 3.68 and a loss tangent of 0.0546 while films of **Poly-4** displayed a dielectric constant of 3.56 with a loss tangent of 0.0302 (Fig. 4a and b). This reduction is attributed to the presence of $-CF_3$ substituents which leads to a decreased overall polarizability. This phenomenon has been observed in various CF_3-containing dielectric polymers,[36] such as fluorinated polyimides.[37–39] Few traditional conjugated ladder polymers have been subjected to thin-film dielectric studies, but a planar poly(-benzimidazobenzophenanthroline) CLP has a dielectric constant of 8.3.[40] Due to the rigid microporous nature of **Poly-3** and **Poly-4**, the lowered dielectric constants would be expected due to the decreased packing density of polymer chains.

Poly-4 achieved substantial discharged energy density, up to 6.54 J cm^{-3} at 650 MV m^{-1} (Fig. 4c). In contrast, **Poly-3** possessed a lower electrical-voltage endurance which limited the film device's capability to withstand higher electric fields, resulting in a maximum discharged energy density of 4.47 J cm^{-3} at an electric field of 550 MV m^{-1}. Further details concerning the dielectric breakdown strength of the films are provided in the ESI.† Under the same electric field, **Poly-3** exhibited an energy efficiency that is inferior to that of **Poly-4** (Fig. 4d), which is likely attributable to the higher polarizability and larger dielectric loss with to the absence of $-CF_3$ groups. With the increase in electric field, the lower energy efficiency of **Poly-3** further decreased. In contrast, **Poly-4** consistently exceeds 85% energy efficiency even at high electric fields of 600–650 MV m^{-1}.

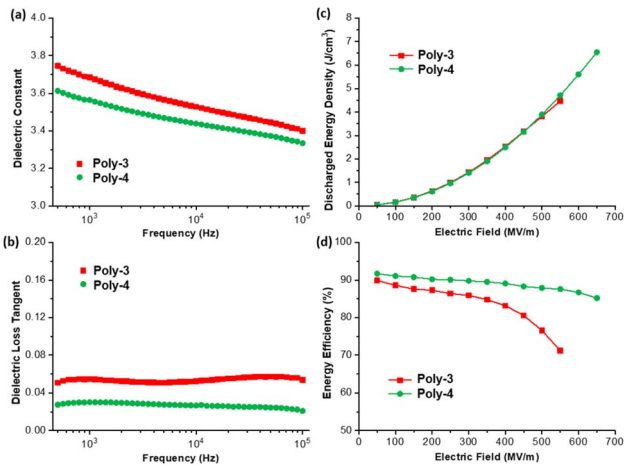

Fig. 4 (a) Frequency-dependent dielectric constant; (b) frequency-dependent dielectric loss tangent; (c) discharged energy density; (d) energy efficiency of COT polymers.

Conclusions

The remarkably efficient dimerization of annulated zirconacycles to generate COT units represents a new pathway to access conjugated ladder polymers, which can exhibit high M_n of nearly 30 kg mol^{-1}. The incorporated COT units in the polymer backbone result in an unusual contorted, rigid ladder structure fully composed of unsaturated carbon atoms. The polymers possess an uncommon combination of properties due to their structure, showcasing intrinsic microporosity, remarkable solubility, and processibility into thin dielectric films which may prove useful for a range of potential applications from gas separation to capacitance.

Data availability

The data supporting this article is included as part of the ESI.†

Author contributions

A. J. R., H. M. B., and T. D. T. conceived of the idea. H. M. B. developed the methodology and A. J. R. used it for materials synthesis. A. J. R. acquired the data for materials synthesis and characterization. H. L. cast thin films and acquired dielectric characterization data. M. Q. acquired porosimetry data. Y. W. acquired X-ray scattering data. A. J. R., H. M. B., H. L., M. Q., Y. W., Y. L., and T. D. T. wrote and edited the manuscript.

Conflicts of interest

There are no conflicts to declare.

Acknowledgements

This work was funded by the National Science Foundation under Grant No. CHE-2103696. Work performed at the Molecular Foundry was supported by the Office of Science, Office of Basic Energy Sciences, of the U. S. Department of Energy under Contract No. DE-AC02-05CH11231. The LBNL Catalysis Laboratory, led by Dr Cooper Citek, provided photophysical instrumentation. The computational work was performed at the UC Berkeley Molecular Graphics and Computation Facility (MGCF), which is supported by the National Institute of Health (Grant No. NIH S10OD023532). The authors thank Dr Hasan Celik, Dr Raynald Giovine, and Pines Magnetic Resonance Center's Core NMR Facility (PMRC Core) for spectroscopic assistance. The instruments used in this work were supported by the PMRC Core. H. L. and Y. L. were supported by the U. S. Department of

Energy, Office of Science, Office of Basic Energy Sciences, Materials Sciences and Engineering Division, under Contract no. DE-AC02-05CH11231 within the Inorganic/Organic Nanocomposites Program (KC3104). The authors would also like to acknowledge Nathalie Co and Alex Wheeler for thoughtful discussions during the assembly of this manuscript.

References

1 Y. C. Teo, H. W. H. Lai and Y. Xia, Saynthesis of Ladder Polymers: Developments, Challenges, and Opportunities, *Chem.–Eur. J.*, 2017, **23**, 14101–14112.
2 Y. Xia, in *Ladder Polymers*, John Wiley & Sons, Ltd, 2023, pp. 1–12.
3 A. M. Robinson and Y. Xia, Regioisomeric Spirobifluorene CANAL Ladder Polymers and Their Gas Separation Performance, *ACS Macro Lett.*, 2024, **13**, 118–123.
4 M. Carta, in *Ladder Polymers*, John Wiley & Sons, Ltd, 2023, pp. 179–218.
5 P. M. Budd, E. S. Elabas, B. S. Ghanem, S. Makhseed, N. B. McKeown, K. J. Msayib, C. E. Tattershall and D. Wang, Solution-Processed, Organophilic Membrane Derived from a Polymer of Intrinsic Microporosity, *Adv. Mater.*, 2004, **16**, 456–459.
6 H. W. H. Lai, F. M. Benedetti, J. M. Ahn, A. M. Robinson, Y. Wang, I. Pinnau, Z. P. Smith and Y. Xia, Hydrocarbon ladder polymers with ultrahigh permselectivity for membrane gas separations, *Science*, 2022, **375**, 1390–1392.
7 J. Lee, Recent Progress in Synthesis of Conjugated Ladder Polymers, *Asian J. Org. Chem.*, 2023, **12**, e202300104.
8 J. Lee, A. J. Kalin, T. Yuan, M. Al-Hashimi and L. Fang, Fully conjugated ladder polymers, *Chem. Sci.*, 2017, **8**, 2503–2521.
9 J. S.-J. Yang and L. Fang, Conjugated ladder polymers: advances from syntheses to applications, *Chem*, 2024, **10**, 1668–1724.
10 T. Ikai, S. Miyoshi, K. Oki, R. Saha, Y. Hijikata and E. Yashima, Defect-Free Synthesis of a Fully π-Conjugated Helical Ladder Polymer and Resolution into a Pair of Enantiomeric Helical Ladders, *Angew. Chem., Int. Ed.*, 2023, **62**, e202301962.
11 S. M. West, D. K. Tran, W. Kaminsky and S. A. Jenekhe, Conjugated Ladder Poly(thienobenzothiazine): Synthesis, Electronic Structure, Optical Properties, and Electrical Conductivity of a Narrow Bandgap p-Type Semiconducting Polymer, *Macromolecules*, 2024, **57**, 8176–8186.
12 S. H. Pun and Q. Miao, Toward Negatively Curved Carbons, *Acc. Chem. Res.*, 2018, **51**, 1630–1642.
13 G. G. Miera, S. Matsubara, H. Kono, K. Murakami and K. Itami, Synthesis of octagon-containing molecular nanocarbons, *Chem. Sci.*, 2022, **13**, 1848–1868.
14 Z. Zhou and M. A. Petrukhina, Planar, curved and twisted molecular nanographenes: reduction-induced alkali metal coordination, *Coord. Chem. Rev.*, 2023, **486**, 215144.
15 Y. Zhang, D. Yang, S. H. Pun, H. Chen and Q. Miao, Merging a Negatively Curved Nanographene and a Carbon Nanoring, *Precis. Chem.*, 2023, **1**, 107–111.
16 S. M. Elbert, O. T. A. Paine, T. Kirschbaum, M. P. Schuldt, L. Weber, F. Rominger and M. Mastalerz, A Negatively Curved Nanographene with Four Embedded Heptagons, *J. Am. Chem. Soc.*, 2024, **146**, 27324–27334.
17 B. Borrisov, G. M. Beneventi, Y. Fu, Z. Qiu, H. Komber, Q. Deng, P. M. Greißel, A. Cadranel, D. M. Guldi, J. Ma and X. Feng, Deep-Saddle-Shaped Nanographene Induced by Four Heptagons: Efficient Synthesis and Properties, *J. Am. Chem. Soc.*, 2024, **146**, 27335–27344.
18 N. M.-W. Wu, M. C. Warndorf, A. Alexander-Katz and T. M. Swager, Oxepine-Based π-Conjugated Ladder/Step-Ladder Polymers with Excited -State Aromaticity, *Macromolecules*, 2024, **57**, 991–1000.
19 F. Schlütter, T. Nishiuchi, V. Enkelmann and K. Müllen, Octafunctionalized Biphenylenes: Molecular Precursors for Isomeric Graphene Nanostructures, *Angew. Chem., Int. Ed.*, 2014, **53**, 1538–1542.
20 Q. Fan, L. Yan, M. W. Tripp, O. Krejčí, S. Dimosthenous, S. R. Kachel, M. Chen, A. S. Foster, U. Koert, P. Liljeroth and J. M. Gottfried, Biphenylene network: A nonbenzenoid carbon allotrope, *Science*, 2021, **372**, 852–856.
21 M. Liu, M. Liu, L. She, Z. Zha, J. Pan, S. Li, T. Li, Y. He, Z. Cai, J. Wang, Y. Zheng, X. Qiu and D. Zhong, Graphene-like nanoribbons periodically embedded with four- and eight-membered rings, *Nat. Commun.*, 2017, **8**, 14924.
22 Y. Liu, Z. Li, M.-W. Wang, J. Chan, G. Liu, Z. Wang and W. Jiang, Highly Luminescent Chiral Double π-Helical Nanoribbons, *J. Am. Chem. Soc.*, 2024, **146**, 5295–5304.
23 T. Ashirov, P. W. Fritz, Y. Lauber, C. E. Avalos and A. Coskun, Fully Conjugated Benzyne-Derived Three-Dimensional Porous Organic Polymers, *Chem.–Eur. J.*, 2023, **29**, e202301053.
24 X. Feng, S. Obermann, X. Zhou, L. A. Guerrero-León, G. Serra, S. Böckmann, Y. Fu, E. Dmitrieva, J.-J. Zhang, F. Liu, A. A. Popov, A. Lucotti, M. R. Hansen, M. Tommasini, Y. Li, P. W. M. Blom and J. Ma, Wavy Graphene Nanoribbons Containing Periodic Eight-Membered Rings for Light-Emitting Electrochemical Cells, *Angew. Chem., Int. Ed.*, 2024, e202415670.
25 S. Ito, M. Wehmeier, J. D. Brand, C. Kübel, R. Epsch, J. P. Rabe and K. Müllen, Synthesis and Self-Assembly of Functionalized Hexa-peri-hexabenzocoronenes, *Chem.–Eur. J.*, 2000, **6**, 4327–4342.
26 Y. Zhang, Q. Tang, Z. Li and K. Zhang, Self-Accelerating Diels–Alder Reaction for Preparing Polymers of Intrinsic Microporosity, *Angew. Chem., Int. Ed.*, 2023, **62**, e202302527.
27 H. M. Bergman, D. D. Beattie, R. C. Handford, E. Rossomme, B. A. Suslick, M. Head-Gordon, T. R. Cundari, Y. Liu and T. D. Tilley, Copper(III) Metallacyclopentadienes *via* Zirconocene Transfer and Reductive Elimination to an Isolable Phenanthrocyclobutadiene, *J. Am. Chem. Soc.*, 2022, **144**, 9853–9858.
28 H. M. Bergman, D. D. Beattie, G. R. Kiel, R. C. Handford, Y. Liu and T. D. Tilley, A sequential cyclization/π-extension strategy for modular construction of nanographenes enabled by stannole cycloadditions, *Chem. Sci.*, 2022, **13**, 5568–5573.

29 P. M. Budd, B. S. Ghanem, S. Makhseed, N. B. McKeown, K. J. Msayib and C. E. Tattershall, Polymers of intrinsic microporosity (PIMs): robust, solution-processable, organic nanoporous materials, *Chem. Commun.*, 2004, 230–231.
30 K. E. Hart, L. J. Abbott and C. M. Colina, Analysis of force fields and BET theory for polymers of intrinsic microporosity, *Mol. Simul.*, 2013, **39**, 397–404.
31 M. Yang, M. Guo, E. Xu, W. Ren, D. Wang, S. Li, S. Zhang, C.-W. Nan and Y. Shen, Polymer nanocomposite dielectrics for capacitive energy storage, *Nat. Nanotechnol.*, 2024, 1–16.
32 F. Le Goupil, V. Salvado, V. Rothan, T. Vidil, G. Fleury, H. Cramail and E. Grau, Bio-Based Poly(hydroxy urethane)s for Efficient Organic High-Power Energy Storage, *J. Am. Chem. Soc.*, 2023, **145**, 4583–4588.
33 C. L. Anderson, H. Li, C. G. Jones, S. J. Teat, N. S. Settineri, E. A. Dailing, J. Liang, H. Mao, C. Yang, L. M. Klivansky, X. Li, J. A. Reimer, H. M. Nelson and Y. Liu, Solution-processable and functionalizable ultra-high molecular weight polymers *via* topochemical synthesis, *Nat. Commun.*, 2021, **12**, 6818.
34 J. Chen, Y. Zhou, X. Huang, C. Yu, D. Han, A. Wang, Y. Zhu, K. Shi, Q. Kang, P. Li, P. Jiang, X. Qian, H. Bao, S. Li, G. Wu, X. Zhu and Q. Wang, Ladderphane copolymers for high-temperature capacitive energy storage, *Nature*, 2023, **615**, 62–66.
35 A. M. M. Hasan, S. Bose, R. Roy, J. D. Marquez, C. Sharma, J. C. Nino, K. O. Kirlikovali, O. K. Farha and A. M. Evans, Electroactive Ionic Polymer of Intrinsic Microporosity for High-Performance Capacitive Energy Storage, *Adv. Mater.*, 2024, **36**, 2405924.
36 G. Maier, Low dielectric constant polymers for microelectronics, *Prog. Polym. Sci.*, 2001, **26**, 3–65.
37 M.-D. Damaceanu and M. Bruma, Local and segmental motion in highly transparent and low-k poly(ether-imide) films, *J. Polym. Res.*, 2014, **22**, 639.
38 X. Wu, J. Cai and Y. Cheng, Synthesis and characterization of high fluorine-containing polyimides with low-dielectric constant, *J. Appl. Polym. Sci.*, 2022, **139**, 51972.
39 W.-L. Qu and T.-M. Ko, Studies of dielectric characteristics and surface energies of spin-coated polyimide films, *J. Appl. Polym. Sci.*, 2001, **82**, 1642–1652.
40 S. Kraner, C. Koerner, K. Leo, E. Bittrich, K.-J. Eichhorn, Y. Karpov, A. Kiriy, M. Stamm, K. Hinrichs and M. Al-Hussein, Dielectric function of a poly(benzimidazobenzophenanthroline) ladder polymer, *Phys. Rev. B: Condens. Matter Mater. Phys.*, 2015, **91**, 195202.